DOI:10.1158/1535-7163.MCT-06-0113

Molecular Cancer Therapeutics

2-Methoxyestradiol suppresses microtubule dynamics and arrests mitosis without depolymerizing microtubules

Kathy Kamath, Tatiana Okouneva, Gary Larson, et al.

Mol Cancer Ther 2006;5:2225-2233. Published online September 19, 2006.

DOI:10.1158/1535-7163.MCT-06-0113

2-Methoxyestradiol suppresses microtubule dynamics and arrests mitosis without depolymerizing microtubules

Kathy Kamath,[1] Tatiana Okouneva,[1] Gary Larson,[1] Dulal Panda,[2] Leslie Wilson,[1] and Mary Ann Jordan[1]

[1]Department of Molecular, Cellular, and Developmental Biology and the Neuroscience Research Institute, University of California, Santa Barbara, California and [2]Indian Institute of Technology Bombay, Mumbai, India

Abstract

2-Methoxyestradiol (2ME2), a metabolite of estradiol-17β, is a novel antimitotic and antiangiogenic drug candidate in phase I and II clinical trials for the treatment of a broad range of tumor types. 2ME2 binds to tubulin at or near the colchicine site and inhibits the polymerization of tubulin *in vitro*, suggesting that it may work by interfering with normal microtubule function. However, the role of microtubule depolymerization in its antitumor mechanism of action has been controversial. To determine the mechanism by which 2ME2 induces mitotic arrest, we analyzed its effects on microtubule polymerization *in vitro* and its effects on dynamic instability both *in vitro* and in living MCF7 cells. *In vitro*, 2ME2 (5–100 μmol/L) inhibited assembly of purified tubulin in a concentration-dependent manner, with maximal inhibition (60%) at 200 μmol/L 2ME2. However, with microtubule-associated protein–containing microtubules, significantly higher 2ME2 concentrations were required to depolymerize microtubules, and polymer mass was reduced by only 13% at 500 μmol/L 2ME2. *In vitro*, dynamic instability was inhibited at lower concentrations. Specifically, 4 μmol/L 2ME2 reduced the mean growth rate by 17% and dynamicity by 27%. In living interphase MCF7 cells at the IC_{50} for mitotic arrest (1.2 μmol/L), 2ME2 significantly suppressed the mean microtubule growth rate, duration and length, and the overall dynamicity, consistent with its effects *in vitro*, and without any observable depolymerization of microtubules. Taken together, the results suggest that the major mechanism of mitotic arrest at the lowest effective concentrations of 2ME2 is suppression of microtubule dynamics rather than microtubule depolymerization *per se*. [Mol Cancer Ther 2006;5(9):2225–33]

Introduction

2-Methoxyestradiol (2ME2) is a novel antiproliferative and antiangiogenic drug in phase I and II clinical trials for the treatment of multiple myeloma; glioblastoma multiforme; and carcinoid, prostate, and breast tumors (1, 2). 2ME2 induces G_2-M arrest and apoptosis in many actively dividing cell types while sparing quiescent cells (3). It also selectively targets endothelial cells of the developing tumor vasculature without affecting preexisting blood vessels and exhibits low toxicity (3).

2ME2 binds to tubulin at or near the colchicine site, it inhibits microtubule assembly, and high concentrations have been shown to depolymerize microtubules in cells (4–6). It also blocks mitosis and inhibits endothelial cell migration (7, 8). Despite its clear effects on microtubules, there is disagreement over the mechanism of action of 2ME2. Some studies have attributed its antimitotic and antiangiogenic effects to depolymerization of microtubules, whereas others indicate that 2ME2 is effective at concentrations that do not significantly depolymerize microtubules. For example, Sattler et al. (8) showed a strong correlation between microtubule depolymerization in endothelial cells and inhibition of endothelial cell adhesion and migration. In addition, concentrations of 2ME2 that inhibited angiogenesis in a mouse orthotopic breast tumor model depolymerized interphase and mitotic microtubules (6). However, Attalla et al. (7) showed that low concentrations of 2ME2 that did not depolymerize microtubules blocked mitosis in Jurkat, A431, and Rat1 cells. Furthermore, in a number of tumor cell lines, the IC_{50} value for proliferation is 10- to 100-fold lower than the concentration required to depolymerize microtubules, and reduction of microtubule polymer mass is not correlated with inhibition of cell proliferation (3). Together, these results have led us to further examine the antiproliferative and antimitotic actions of 2ME2.

Microtubules are dynamic polymers that can alternate between phases of slow growth and rapid shortening through continuous tubulin addition and loss at their ends, a process called dynamic instability (9). In cells, the rates of microtubule growth and shortening, the frequencies with which microtubules switch between growth and shortening, and the overall dynamicity of microtubules are tightly controlled spatially and temporally (10). The precise regulation of dynamic instability is critical in mitosis for the bipolar attachment of microtubules to each chromosome,

Received 2/28/06; revised 7/14/06; accepted 7/26/06.

Grant support: Grants CA57291 (M.A. Jordan), NS13560 (L. Wilson), and fellowship SB050106 (K. Kamath).

The costs of publication of this article were defrayed in part by the payment of page charges. This article must therefore be hereby marked advertisement in accordance with 18 U.S.C. Section 1734 solely to indicate this fact.

Requests for reprints: Kathy Kamath, Department of Molecular, Cellular, and Developmental Biology, University of California, Santa Barbara, Bio II Room 3106, Santa Barbara, CA 93106. Phone: 805-893-8057. E-mail: kamath@lifesci.ucsb.edu

doi:10.1158/1535-7163.MCT-06-0113

DOI:10.1158/1535-7163.MCT-06-0113

alignment of chromosomes at the metaphase plate, signaling at the metaphase/anaphase transition, and chromosome separation at anaphase (11, 12). Disruption of any of these processes can lead to mitotic arrest, aneuploidy, and cell death (13).

Another potential mechanism by which 2ME2 might exert its antimitotic effects is through suppression of microtubule dynamics. Several microtubule-targeted drugs, including paclitaxel and Vinca alkaloids, potently suppress microtubule dynamics *in vitro* at lower concentrations than those required to significantly alter microtubule polymer mass (14, 15). Thus, we hypothesized that 2ME2 also might induce mitotic arrest by suppressing microtubule dynamics. To test this hypothesis, we analyzed the effects of 2ME2 on microtubule dynamic instability and polymer mass *in vitro* over a range of concentrations, and we determined the intracellular drug concentration and its effects on microtubule dynamic instability in cells. We found that 2ME2 induced a concentration-dependent suppression of microtubule dynamic instability and a reduction of polymer *in vitro.* In MCF7 cells, at the IC_{50} for mitotic arrest, 2ME2 significantly suppressed microtubule dynamic instability specifically by reducing microtubule growth parameters and increasing the time microtubules spent in a phase of pause or attenuation. These changes resulted in an overall reduction in microtubule dynamicity with no detectable depolymerization. In addition, 2ME2 concentrated 13-fold in cells and was rapidly lost from cells when 2ME2 was removed from the medium, an observation that has important implications for the use of 2ME2 as an anticancer therapy.

Materials and Methods

All materials were purchased from Sigma (St. Louis, MO) unless otherwise noted. Stock solutions of 2ME2 and [^{3}H]2ME2 (Sigma and EntreMed, Inc., Rockville, MD; 10 mmol/L and 1.2 μmol/L, respectively) were prepared in DMSO for most experiments and in 20% DMSO and 80% ethanol for microtubule-associated protein (MAP)–rich microtubule depolymerization experiments. Podophyllotoxin (5 mmol/L) was dissolved in DMSO. Vinblastine (100 μmol/L) was dissolved in water. Microtubule protein was purified from bovine brain by three cycles of polymerization and depolymerization (16). Tubulin was purified from microtubule protein by phosphocellulose chromatography (17). Protein concentrations were determined by the Bradford assay (18) using bovine serum albumin as the standard, drop frozen in liquid nitrogen, and stored at −70°C.

Determination of Effects on Microtubule Polymer Mass of MAP-Containing Tubulin *In vitro*

Microtubule protein (2.75 mg/mL; ref. 16) was assembled to steady-state [in 100 mmol/L PIPES containing 1 mmol/L EGTA and 1 mmol/L $MgSO_4$ (PEM100) and 1 mmol/L GTP, 35°C for 45 minutes] containing 2ME2 (final drug concentrations of 1–500 μmol/L). Final DMSO and ethanol concentrations were adjusted to 1% and 5%, respectively. Concentrations of 2ME2 ≤ 5 μmol/L had no effect on microtubule polymer mass, and thus 20 to 500 μmol/L 2ME2 was used for most of the experiments. Incubation with 2ME2 was carried out for 30 minutes, at which time microtubule depolymerization was maximal, and microtubules were centrifuged at 35°C for 30 minutes and the supernatant was removed from the pellets. Microtubule pellets were solubilized overnight in 0.2 mol/L NaOH and the protein concentrations of supernatants and pellets were determined. We examined the effects of 10 μmol/L vinblastine on depolymerization ± 1% DMSO to test whether the DMSO that was necessary in the 2ME2 experiments might influence the depolymerization level. We found no effect of the DMSO on the depolymerization level. Podophyllotoxin (20 μmol/L) was used as a positive control.

Determination of Effects on Microtubule Polymer Mass of MAP-Free Tubulin *In vitro*

Purified bovine brain tubulin (3.0 mg/mL) was assembled in the presence of 2ME2 (final drug concentrations of 1–500 μmol/L) in 100 mmol/L PIPES containing 1 mmol/L EGTA, 1 mmol/L $MgSO_4$ (PEM100), and 1 mmol/L GTP, at 30°C. Final DMSO and ethanol concentrations were adjusted to ≤1% and 5%, respectively, and assembly was monitored by light scattering at 350 nm in a Beckman DU 640 spectrophotometer. Microtubules were centrifuged at 20,000 rpm for 60 minutes, at 30°C, in a Sorvall RC5B plus centrifuge with an SS-34 rotor. Supernatants were removed from pellets, and the protein concentrations of the pellets were determined.

Cell Culture. MCF7 breast carcinoma cells (American Type Culture Collection, Manassas, VA) stably transfected with green fluorescent protein (GFP)-α-tubulin (Clontech, Palo Alto, CA) were cultured in DMEM supplemented with nonessential amino acids, 0.1% penicillin/streptomycin, 10% fetal bovine serum (Hyclone, Logan, UT), and 0.4 mg/mL G418 (Biowhittaker, Rockland, ME) at 37°C in 5% CO_2. Transfection of MCF7 cells with GFP-α-tubulin was carried out as described previously (19).

Determination of Half-Maximal (IC_{50}) Mitotic Arrest. To evaluate mitotic indices, cells were plated at a concentration of 6×10^4/2 mL into six-well plates. After 48 hours, cells were incubated in the absence or presence of 2ME2 at concentrations ranging from 100 nmol/L to 30 μmol/L for 20 hours. To collect both floating and attached cells, medium was collected; attached cells were rinsed with Versene (137 mmol/L NaCl, 2.7 mmol/L KCl, 1.5 mmol/L KH_2PO_4, 8.1 mmol/L Na_2HPO_4, and 0.5 mmol/L EDTA), detached by trypsinization, and added back to the medium. Cells were collected by centrifugation and fixed with 10% formalin for 30 minutes, permeabilized in ice-cold methanol for 10 minutes, and stained with 4′,6-diamidino-2-phenylindole to visualize nuclei. Results are the mean and SE of seven experiments in each of which 500 cells were counted for each concentration. The mitotic IC_{50} is the drug concentration that induced one half of the maximal mitotic accumulation.

Image Acquisition and Analysis of Microtubule Dynamics *In vitro*. Tubulin (1.2 mg/mL) was polymerized to steady-state using *Strongylocentrotus purpuratus* axoneme

DOI:10.1158/1535-7163.MCT-06-0113

fragments as seeds for assembly. The dynamics at the plus ends of microtubules were recorded by video-enhanced differential interference contrast microscopy using a Zeiss IM35 inverted microscope and Zeiss Planapo (numerical aperture 1.4, ×63 objective) and a stage maintained at 35°C to 37°C as described previously (20). The microtubule lengths were measured every 3 to 5 seconds, graphed as microtubule length versus time, and analyzed using real-time measurement software (21). Growth and shortening events were determined by least-square regression analysis. A microtubule was considered to be in a growth phase if it increased in length by >0.2 μm at a rate >0.15 μm/min and in a shortening phase if it shortened by >0.2 μm at a rate >0.3 μm/min. The frequency at which microtubules switched from phases of growth or attenuation to shortening (catastrophe) or from shortening to growth or attenuation (rescue) and the percentages of time the population of microtubules spent growing, shortening, and attenuated were determined as described previously (20). Dynamicity was calculated as the total rate of measurable tubulin exchange at the microtubule ends (17).

Image Acquisition and Analysis of Microtubule Dynamics In Living Cells. Cells were prepared for analysis of interphase microtubule dynamics as described previously (19). Briefly, MCF7 cells expressing GFP-tubulin were grown for 48 hours on coverslips (pretreated with poly-lysine, laminin, and fibronectin to induce cell flattening) and then incubated in the presence or absence of 2ME2 for 6 hours. Control cells were incubated with an equivalent concentration of DMSO alone. Cells were transferred to recording medium [DMEM lacking phenol red and supplemented with 25 mmol/L HEPES, 3.5 g/L glucose, and Oxyrase (Oxyrase, Inc., Mansfield, OH) to inhibit photobleaching and prevent photodamage] containing 1.2 μmol/L 2ME2. Analysis was carried out 15 minutes to 2 hours after sealing coverslips in a double coverslip chamber. Thirty-one time-lapse images of each cell were acquired at 4-second intervals using a Hamamatsu ORCA II digital camera (Middlesex, NJ) driven by Metamorph software (Universal Imaging, Media, PA) on a Nikon Eclipse E800 fluorescence microscope with a forced air heating chamber maintaining the stage and objective at 36 ± 1°C. The positions of the plus ends of microtubules over time were tracked using the Track Points function of Metamorph (Universal Imaging), graphed as microtubule length over time (life history plots) and the variables of microtubule dynamics were determined. The criteria used to analyze microtubule dynamics in living cells are described in detail in ref. (19). We also found that it was critical to maintain the 2ME2 concentration in the medium during analysis of microtubule dynamics in cells. When 2ME2 was not included in the recording medium, there was no significant suppression of microtubule dynamics, consistent with rapid loss of 2ME2 from cells (see Results).

Immunofluorescence Microscopy. MCF7 cells were prepared for immunofluorescence microscopy as for analysis of microtubule dynamics except that coverslips were pretreated with poly-lysine but not laminin or fibronectin. Cells were incubated with 0, 1.2, or 10 μmol/L 2ME2 for 20 hours; fixed in 10% formalin for 30 minutes at room temperature; and permeabilized in methanol at −20°C for 10 minutes. Nonspecific antibody staining was blocked with 20% normal goat serum in PBS containing 1% bovine serum albumin and cells were incubated with DM1a anti-α-tubulin antibody (Sigma) followed by CY3 goat anti-mouse secondary antibody (Jackson Immunolaboratories, Westgrove, PA) to visualize microtubules. Nuclei were stained with 4′,6-diamidino-2-phenylindole and coverslips were mounted with Prolong Antifade (Molecular Probes, Eugene, OR).

Analysis of Drug Uptake and Efflux. MCF7 cells were seeded into poly-lysine-treated scintillation vials (1×10^5 cells, 1 mL). After 48 hours, medium was replaced with fresh medium containing 1.2 μmol/L [^{3}H]2ME2 (specific activity 200–500 Ci/mol) or unlabeled 2ME2 (for determination of cell number). Medium was removed from vials at 15 and 30 seconds; 1, 5, and 10 minutes; and 1, 2, 5, and 20 hours after drug addition. Cells were then rapidly rinsed twice with 1 mL PBS and intracellular 2ME2 was determined by scintillation counting. Background radioactivity was determined by treating vials containing only radiolabeled medium (no cells) as above. Potential nonspecific binding to cells was determined by extrapolation of the linear regression of the initial rate of uptake (15 seconds–1 minute) to time 0 (3.7 μmol/L). The intracellular drug concentration was then determined by dividing the moles of intracellular 2ME2 by the average cell volume times the number of cells per vial. The mean cell volume was calculated from the mean diameter of cells rounded up after trypsinization ($n = 38$, mean cell volume = 3.2×10^{-12} L). Cell number was determined at the time of addition and 20 hours after incubation in 1.2 μmol/L 2ME2 by manual cell counting using a hemacytometer. Additionally, after 20 hours, cells were washed with 1 mL PBS for 1 minute and 5 minutes to determine how readily 2ME2 is washed out of cells. We also did drug uptake experiments using the same seeding conditions as we used in the microtubule dynamics experiments (3×10^4 cells/mL × 2 mL). These conditions yielded a slightly higher intracellular drug concentration. All time points were measured in duplicate, and results are the mean and SD of five experiments.

Results

Effects of 2ME2 on the Assembly and Dynamics of Purified Microtubules *In vitro*

Microtubules were assembled from MAP-free bovine brain tubulin in the presence of a range of concentrations of 2ME2 (1–500 μmol/L) or in its absence, and assembly was monitored by light scattering. The percentage of tubulin in microtubule polymer was determined by centrifugation of microtubules and analysis of protein content of the pellets. 2ME2 inhibited the assembly of purified bovine brain tubulin in a concentration-dependent manner with half-maximal inhibition at ~40 μmol/L and maximal inhibition at 200 μmol/L (Fig. 1).

DOI:10.1158/1535-7163.MCT-06-0113

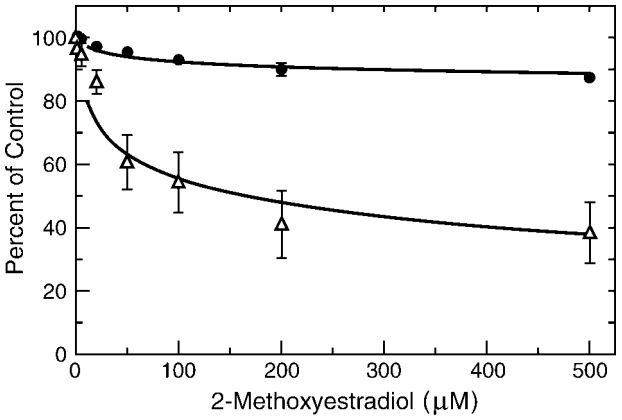

Figure 1. Effects of 2ME2 on the polymer mass of steady-state MAP-rich (●) and MAP-free tubulin (△) *in vitro*. For MAP-rich tubulin, microtubule protein (2.75 mg/mL) was assembled to steady-state and 2ME2 (5 – 500 μmol/L) or vehicle alone was added and microtubules were incubated for an additional 30 min. Protein content of pellets after centrifugation of remaining microtubules was determined. In controls, ~90% of the protein was in polymer. Podophyllotoxin (20 μmol/L) induced a 25% reduction in polymer mass (not shown). For MAP-free conditions, tubulin (3.0 mg/mL) was assembled in the presence of 2ME2 (1 – 500 μmol/L) and assembly was monitored by light scattering. Microtubules were centrifuged, the supernatants were removed, and the protein content of the pellets was determined. Results are reported as percentage of control. *Points,* mean of five experiments; *bars,* SD (for MAP-rich tubulin) and SE (for MAP-free tubulin).

Because microtubules in cells are associated with many microtubule-interacting proteins, we also analyzed the ability of 2ME2 to depolymerize microtubules assembled from bovine brain tubulin containing MAPs, a system that may more closely reflect conditions in cells. Microtubule protein was assembled to steady-state and 2ME2 (20–500 μmol/L) or vehicle alone was added and incubated for an additional 30 minutes. Microtubule mass was determined as described above. Significantly higher concentrations of 2ME2 were required to reduce the mass of MAP-containing microtubules compared with microtubules assembled from MAP-free tubulin. As shown in Fig. 1, 50 μmol/L 2ME2 reduced the microtubule protein polymer mass by only 5%, whereas this concentration inhibited polymerization of MAP-free tubulin by 40%. 2ME2 at 500 μmol/L reduced polymer mass by only 12.5%.

To determine the effects of 2ME2 on microtubule dynamic instability, MAP-free bovine brain tubulin was assembled to steady-state and dynamic instability was analyzed in the presence or absence of 2ME2 (4–50 μmol/L) by video-enhanced differential interference contrast microscopy. MAP-free microtubules were used because, *in vitro*, MAPs suppress microtubule dynamic instability so potently that it is difficult to study the effects of drugs. The changes in length at the plus ends of microtubules were determined and graphed as a function of time to create microtubule life history plots from which the parameters of microtubule dynamics were derived (Materials and Methods). We found that 2ME2 significantly suppressed microtubule dynamic instability in a concentration-dependent manner (Table 1; Fig. 2A–C). For example, the mean microtubule growth rate was suppressed by 42% and 56% at concentrations of 20 and 50 μmol/L 2ME2, respectively. 2ME2 also induced a concentration-dependent decrease in the percentage of time microtubules spent growing and an increase in the percentage of time microtubules spent attenuated. The frequencies with which microtubules alternate from phases of growing or attenuation to shortening (catastrophe) or from shortening to growing or attenuation (rescue) also reflect the overall dynamics of a population of microtubules. The time-based catastrophe frequency was also reduced by 2ME2 in a concentration dependent manner. As a result of these changes, dynamicity (a measure of the total tubulin

Table 1. Effects of 2ME2 on the dynamic instability of steady-state MAP-free microtubules *in vitro*

	[2ME2] (μmol/L)			
	0	4	20	50
Parameter				
Growth rate (μm/min)	0.52 ± 0.06	0.43 ± 0.03	**0.3 ± 0.03**	**0.23 ± 0.02**
Growth length (μm)	1.3 ± 0.2	1.2 ± 0.2	0.8 ± 0.1	0.8 ± 0.1
Shortening rate (μm/min)	28.0 ± 3.4	26.5 ± 3.9	18.3 ± 4.2	*
Shortening length (μm)	6.9 ± 0.8	4.4 ± 0.8	4.7 ± 0.8	1.4 ± 0.9
Catastrophe frequency (min^{-1})	0.16 ± 0.05	0.13 ± 0.04	0.10 ± 0.03	0.02 ± 0.01
Rescue frequency (min^{-1})	0.9 ± 0.5	1.4 ± 0.7	0.6 ± 0.3	0.4 ± 0.2
Dynamicity (μm/min)	1.5	1.1	0.57	0.14
Percentage (%) of time spent:				
Growing	88.6	84.4	73.9	51.3
Shortening	4.2	4.0	5.0	3.7
Paused	7.2	11.6	21.2	45.0

NOTE: Values in bold are significant at ≥99% confidence interval by Student's *t* test. Catastrophe and rescue frequency and dynamicity are calculated from the population of microtubules and thus statistical analysis cannot be done on these variables.
*Shortening events were rare at this concentration and, thus, the shortening rate could not be accurately calculated.

DOI:10.1158/1535-7163.MCT-06-0113

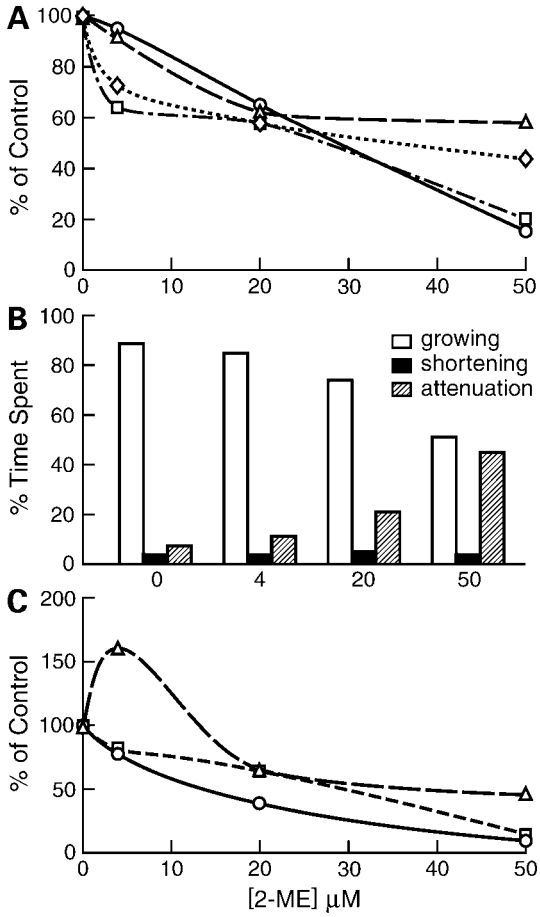

Figure 2. Concentration dependence for the suppression of microtubule dynamic instability *in vitro* by 2ME2. 2ME2 induced a concentration-dependent (**A**) suppression of the microtubule growth (◇) and shortening rates (○), and growth (△) and shortening lengths (□); (**B**) increased the percentage of time microtubules spent attenuated; and (**C**) decreased the dynamicity (○) and time-based catastrophe frequency (□). The time-based rescue frequency (△) increased at 4 μmol/L and was suppressed at higher concentrations.

exchange at microtubule plus ends) was reduced by 62% and 90% at 20 and 50 μmol/L, respectively.

2ME2 Suppresses Microtubule Dynamic Instability in Living Interphase Cells at Concentrations that Arrest Mitosis

The ability of 2ME2 to suppress microtubule dynamic instability *in vitro* led us to ask whether 2ME2 also suppresses dynamic instability in living cells in concert with mitotic arrest. Mitosis was arrested in MCF7 cells in a 2ME2 concentration-dependent manner. In untreated controls, mitotic cells represented 2.5% of the total population (Fig. 3). In cells incubated with 0.6 μmol/L 2ME2 for 20 hours, 6.8% of the cells were in mitosis, and the percentage of mitotic cells reached a maximum of 30% at 3 μmol/L 2ME2. Mitotic arrest was half-maximal at 1.2 μmol/L 2ME2 (mitotic IC_{50}).

The effects of 2ME2 on dynamic instability were determined in living interphase MCF7 cells expressing GFP-tubulin as a marker to visualize microtubules. Cells were incubated with or without 2ME2 at the mitotic IC_{50} (1.2 μmol/L) for 6 hours. This time period is sufficient to achieve an equilibrium intracellular drug concentration (see drug uptake below). Fluorescence time-lapse images of GFP-labeled microtubules were captured and the changes in microtubule length were graphed as life history plots from which the parameters of dynamic instability were determined. As shown in Table 2, at the mitotic IC_{50}, 2ME2 reduced the mean microtubule growth rate (−26%), growth duration (−30%), growth length (−57%), and the time-based catastrophe frequency (−41%), and significantly increased the percentage of time microtubules spent paused (+21%), resulting in an overall reduction in microtubule dynamicity of 43%. These effects are similar to those observed at 4 μmol/L 2ME2 *in vitro*, indicating that both *in vitro* and in cells, 2ME2 suppresses microtubule dynamics and, in cells, suppression occurs in concert with mitotic arrest.

2ME2 Concentrates in Cells, Rapidly Reaches Equilibrium, and Is Readily Washed Out

The time course and extent of uptake of 1.2 μmol/L [^{3}H]2ME2 into MCF7 cells is shown in Fig. 4 and its efflux upon washing with drug-free PBS is shown in the inset. 2ME2 reached an intracellular equilibrium concentration (15.9 μmol/L) <1 hour after adding drug, under the conditions of the experiment (1×10^5 cells/mL, 1 mL). Subtraction of potential nonspecific binding of 2ME2 to cells (3.7 μmol/L; see Materials and Methods) resulted in an intracellular concentration of 12.2 μmol/L. Thus, it was concentrated ~10-fold and the concentration was maintained unaltered over 20 hours (Fig. 4). The seeding density and medium volume affected the equilibrium concentration to some degree. Under conditions that recapitulated our microtubule dynamics experiments (3×10^4 cells/mL, 2 mL) the intracellular concentration was 33 μmol/L (data not shown).

Upon removal of drug-containing medium and addition of 1 mL PBS for 1 minute, the intracellular drug concentration was reduced to 8.7 μmol/L, and after 5 minutes it was reduced to 6.5 μmol/L. These concentrations

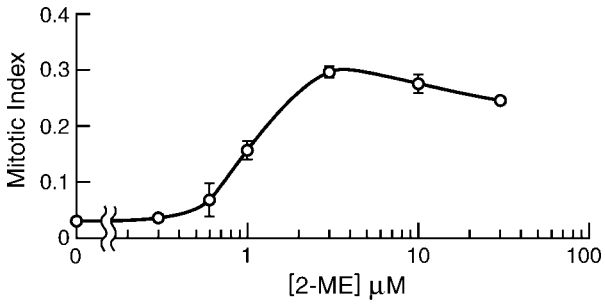

Figure 3. Percentage of cells in mitosis in the presence of 0 to 30 μmol/L 2ME2. 2ME2 maximally inhibited mitosis at concentrations ≥3 μmol/L. Half-maximal mitotic arrest (IC_{50}) was calculated as 1.2 μmol/L 2ME2. *Points,* mean of seven experiments; *bars,* SE.

DOI:10.1158/1535-7163.MCT-06-0113

Table 2. Effects of 2ME2 on microtubule dynamics in living cells at the mitotic IC_{50}

	Control	2ME2 mitotic IC_{50} (1.2 μmol/L)	Percentage change (%)
Variable			
Growth rate (μm/min)	12.3 ± 3.8	9.1 ± 4.4	−26
Growth duration (min)	0.33 ± 0.22	0.23 ± 0.17	−30
Growth length (μm)	4.1 ± 3.3	1.8 ± 1.4	−57
Shortening rate (μm/min)	30.6 ± 12.2	**33.3 ± 14.4**	NS
Shortening duration (min)	0.18 ± 0.09	**0.18 ± 0.08**	NC
Shortening length (μm)	6.0 ± 4.2	**6.1 ± 3.8**	NC
Pause duration (min)	0.26 ± 0.23	**0.31 ± 0.26**	NS
Catastrophe frequency/MT/min	1.8 ± 1.0	1.0 ± 1.0	−41
Rescue frequency/MT/min	4.8 ± 3.1	**4.0 ± 3.3**	−17
Catastrophe frequency/MT/μm	0.41 ± 0.40	**0.44 ± 0.44**	NS
Rescue frequency/MT/μm	0.18 ± 0.16	**0.16 ± 0.19**	NS
Dynamicity/MT (μm/min)	11.6 ± 4.3	6.6 ± 3.2	−43
Percentage (%) of time spent:			
Growing	40.0	27.7	−12
Shortening	22.9	13.8	−9
Paused	37.1	58.5	+21
MTs/cells	49/8	65/15	

NOTE: Values are the mean ± SD except for percentage of time spent in each phase, which represents the behavior of the entire population of microtubules. Values in bold type are statistically significant at ≥99% confidence level by Student's *t* test.
Abbreviations: MT, microtubule; NC, no change; NS, not significant.

would be further reduced to 5 and 2.8 μmol/L respectively, assuming that nonspecific binding to cells is maintained at 3.7 μmol/L after washout. Thus, 1.2 μmol/L 2ME2 is rapidly taken up and concentrated in cells, and a large portion of it is rapidly lost from cells upon removal of drug from the medium.

The Effects of 2ME2 on Microtubule Organization in Cells

To further characterize the effects of 2ME2 on microtubule arrangement, we examined cells incubated with 2ME2 by immunofluorescence microscopy. The effects of 2ME2 (1.2–20 μmol/L) on the microtubule arrays of fixed cells, or of live cells expressing GFP-tubulin, are shown in Figs. 5 and 6. In interphase cells incubated with 2ME2 at the mitotic IC_{50} (Fig. 5B) and eight times the mitotic IC_{50} (Fig. 5C), the microtubule network was similar to that of controls [compare 5B (1.2 μmol/L) and C (10 μmol/L) with 5A (control)]. Microtubules emanated from a central microtubule-organizing center (not shown), were well spread and not bundled or contorted and extended to the cell periphery, and there was no evidence of microtubule depolymerization (Fig. 5A–C). At 20 μmol/L 2ME2 (Fig. 5D), however, the mass of microtubule polymer was decreased compared with controls, as indicated by the increased diffuse GFP-tubulin at the cell periphery.

Mitotic arrest that is associated with suppression of microtubule dynamics by many drugs, including the Vinca alkaloids and paclitaxel, is characterized by spindle abnormalities including uncongressed chromosomes, multipolar spindles, and other aberrant spindle morphologies (14, 22, 23). In addition to its effects on microtubule dynamics and polymer mass, 2ME2 also induced spindle abnormalities. In control mitotic cells, most spindles were bipolar (Fig. 6A and B) with all the chromosomes congressed to a compact metaphase plate (Fig. 6A). At the mitotic IC_{50} (1.2 μmol/L, Fig. 6C–E), most of the spindles were bipolar; however, one or more uncongressed chromosomes were often located at the poles (Fig. 6C). In a large percentage of the abnormal spindles, unaligned

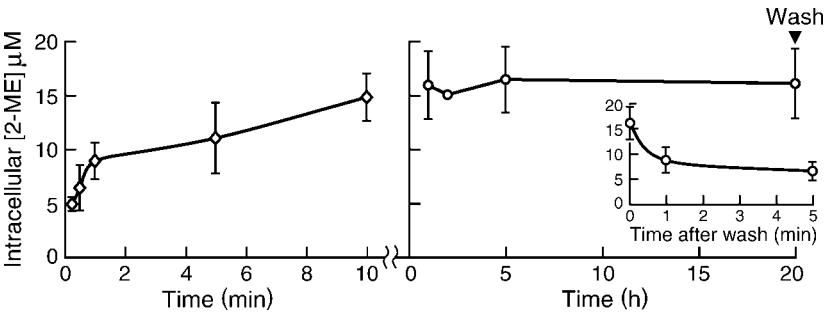

Figure 4. Time course of uptake of 2ME2 into cells and its retention upon washing. Cells were incubated with 1.2 μmol/L [^{3}H]2ME2 (mitotic IC_{50}), and intracellular levels were measured at the indicated times (Materials and Methods). *Inset,* after 20 h, the medium was removed and replaced with 1 mL PBS for 1 and 5 min to determine the rate of 2ME2 washout from cells. *Points,* mean of five experiments; *bars,* SD. The graph reflects the intracellular 2ME2 concentration before subtraction of potential nonspecific cell binding (3.7 μmol/L; see Materials and Methods).

DOI:10.1158/1535-7163.MCT-06-0113

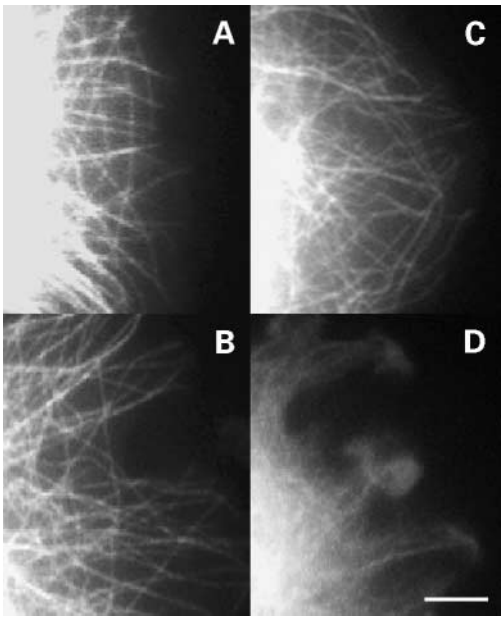

Figure 5. GFP-labeled microtubules in living interphase MCF7 cells. Control cells (**A**) and cells incubated with 1.2 (**B**) or 10 μmol/L 2ME2 (**C**) exhibited a normal microtubule organization with no evidence of microtubule depolymerization. The microtubule network was significantly depolymerized in interphase cells incubated with 20 μmol/L 2ME2 (**D**). Bar, 5 μm.

chromosomes were clustered at only one pole and there were more astral microtubules emanating from this pole compared with the other pole (Fig. 6C, *arrows*). Asymmetrical or lopsided spindles were prominent in both fixed and living mitotic cells at the mitotic IC_{50} (Fig. 6D). At eight times the mitotic IC_{50} (10 μmol/L 2ME2), spindles were not bipolar but were completely abnormal and contained multiple tiny asters composed of short microtubules with a few chromosomes clustered around each aster (Fig. 6F and G). In contrast, interphase microtubule arrays (Fig. 5C) appeared normal at this concentration. Thus, mitotic spindles seem to be significantly more sensitive to the effects of 2ME2 than interphase microtubule arrays.

Discussion

Both *in vitro* and in living cells, we found that 2ME2 suppresses microtubule dynamic instability. In cells, concentrations of 2ME2 that induced mitotic arrest suppressed dynamic instability with no accompanying detectable microtubule depolymerization. Thus, like other microtubule-targeted drugs, suppression of microtubule dynamics by 2ME2 seems to be the most potent mechanism of mitotic arrest. In addition, because 2ME2 inhibits endothelial cell capillary formation (a critical step in angiogenesis) at significantly lower concentrations than those required to inhibit endothelial cell proliferation (24), our results further suggest that the antiangiogenic effects of 2ME2 are unlikely to result from microtubule depolymerization.

Both *in vitro* and in cells, the most potent action of 2ME2 was to suppress parameters associated with microtubule growth, resulting in an overall decrease in microtubule dynamicity. *In vitro*, 4 μmol/L 2ME2 suppressed the mean growth rate by 27% compared with 26% reduction in cells at the mitotic IC_{50}. Dynamicity was reduced by 22% and 43% *in vitro* and in cells, respectively.

At the IC_{50} for mitotic arrest (1.2 μmol/L), the intracellular drug concentration was 10- to 30-fold higher (12–33 μmol/L) than the medium concentration. No significant microtubule depolymerization was detectable either by immunofluorescence microscopy of fixed cells at the IC_{50} or during live cell imaging. *In vitro*, 2ME2 only weakly affected the polymer mass of steady-state MAP-rich microtubules with a reduction in microtubule polymer of only 12.5% at 500 μmol/L. The reduction in microtubule polymer mass at 20 and 50 μmol/L 2ME2 (approximately equivalent to the intracellular concentration at the mitotic

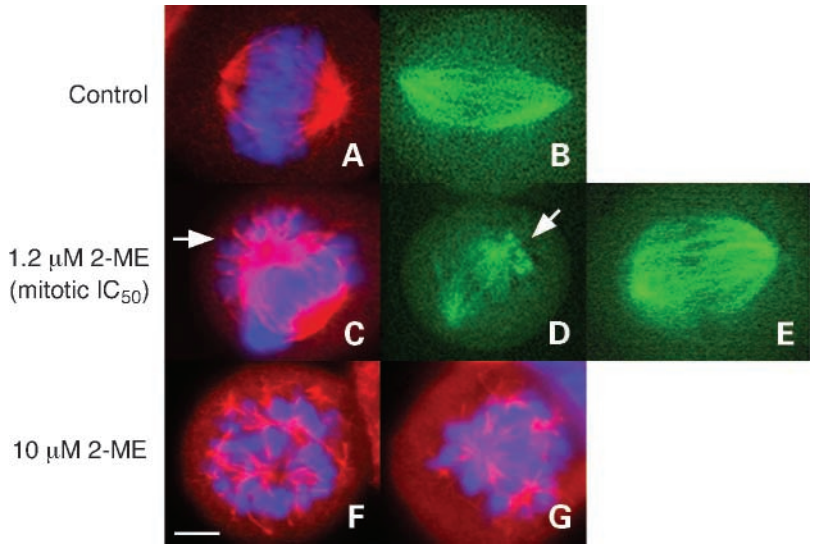

Figure 6. Immunofluorescence images of fixed and stained mitotic cells (*red,* tubulin; *blue,* nuclei; **A, C, F,** and **G**) and living mitotic cells expressing GFP-tubulin (*green*; **B, D,** and **E**) in the presence and absence of 2ME2. In control mitotic cells (**A** and **B**), spindles were bipolar. However, in the presence of 1.2 μmol/L 2ME2, one to several chromosomes were often located asymmetrically at one of the poles (*arrows* in **C**) and the spindles were lopsided with increased microtubule density and abnormal organization at the pole containing the uncongressed chromosomes (*arrows* in **C** and **D**). Mitotic cells incubated with 10 μmol/L 2ME2 (**F** and **G**), contained multiple asters and chromosomes were clustered around each aster. Bar, 5 μm.

DOI:10.1158/1535-7163.MCT-06-0113

IC_{50}) was ~3% and 5%, respectively. Although 20 to 50 μmol/L 2ME2 significantly inhibited assembly of MAP-depleted microtubules *in vitro*, in cells, microtubules are not MAP-free but are associated with large numbers of MAPs. In addition, drugs in cells may be sequestered by cellular organelles; thus, the effects of a given drug concentration in cells may not be equivalent to its effects *in vitro*. Taken together, the data suggest that MAPs stabilize microtubules against depolymerization by 2ME2. They further support the hypothesis that the primary mechanism of mitotic arrest at low concentrations of 2ME2 is suppression of microtubule dynamics.

Of great significance is the observation that although 2ME2 shares the ability to suppress microtubule dynamics with several other successful chemotherapeutic drugs, including the Vinca alkaloids, unlike these drugs, it is relatively nontoxic and does not seem to have the frequent dose-limiting side effects associated with other microtubule-targeted drugs. The low toxicity of 2ME2 may, in part, be related to its rapid reversibility.

Effects of 2ME2 on Spindle Morphology

In addition to its effects on microtubule dynamics and polymer mass, 2ME2 also induced many spindle abnormalities including frequent asymmetrical spindles. One possible explanation for spindle asymmetry is that 2ME2 may bind to components of the centrioles or centrosomes. Centrioles contain several additional tubulin species, including γ, δ, and ε-tubulin, as well as the αβ-tubulin that makes up the nondynamic triplet microtubules within centrioles. Because the centrioles at the two poles are not identical, we tested whether 2ME2 might bind to γ-tubulin and thus possibly influence pole asymmetry. However, no binding of 2ME2 to γ-tubulin was detected.[3] ε-Tubulin is primarily localized to the mother of the oldest centriolar pair and is only recruited to the newer centrosome after S phase (25). It is conceivable that 2ME2 could selectively inhibit the interaction of ε-tubulin with additional centrosomal components selectively at the older centrosome, or interfere with its proper recruitment to the newer one. In support of the latter hypothesis, ε-tubulin has been shown to anchor microtubules at the centrosome and interference with this activity could account for the observation that fewer microtubules emanate from one of the two spindle poles. Determining whether 2ME2 binding to centrioles or to these additional tubulin species alters the localization of centrosomal proteins will be an important step in unraveling its actions in cells.

In summary, the ability of 2ME2 to depolymerize MAP-rich microtubules *in vitro* required significantly higher concentrations than those that affected MT dynamics either *in vitro* or in cells. Our results support the hypothesis that at its lowest effective concentrations, 2ME2 induces mitotic arrest by suppressing microtubule dynamics particularly by suppressing microtubule growth parameters and increasing the percentage of time microtubules spend in a paused state, thereby interfering with chromosome congression and cell division. Higher concentrations of 2ME2 prevent mitotic progression by inhibiting microtubule polymerization and normal spindle assembly, resulting in tiny multipolar spindles. The asymmetrical spindles we observed even at low concentrations of 2ME2 suggest that it may have additional actions at the centrosome that contribute to both its antimitotic and antiangiogenic effects. In addition, rapid uptake and loss of 2ME2 from cells suggests that it may be therapeutically necessary to maintain its concentration in tumors by continuous or frequent dosing. Our findings are consistent with clinical results indicating that optimal antitumor activity is achieved with three to four times per day oral dosing.[4]

[3] K. Kamath, L. Wilson, and M.A. Jordan, unpublished results.
[4] T. LaVallee, EntreMed, Inc., personal communication.

Acknowledgments

We thank Herb Miller for the preparation of purified bovine brain tubulin and Michele Moritz (University of California, San Francisco, San Francisco, CA) for providing purified γ tubulin.

References

1. Sweeney C, Liu G, Yiannoutsos C, et al. phase II multicenter, randomized, double-blind, safety trial assessing the pharmacokinetics, pharmacodynamics, and efficacy of oral 2-methoxyestradiol capsules in hormone-refractory prostate cancer. Clin Cancer Res 2005;11:6625–33.

2. Mooberry S. Mechanism of action of 2-methoxyestradiol:new developments. Drug Resist Updat 2003;6:355–61.

3. Pribluda VS, Gubish ER, Jr., LaVallee TM, Treston A, Swartz GM, Green SJ. 2-Methoxyestradiol: an endogenous antiangiogenic and antiproliferative drug candidate. Cancer Metastasis Rev 2000;19:173–9.

4. D'Amato R, Lin C, Flynn E, Folkman J, Hamel E. 2-Methoxyestradiol, an endogenous mammalian metabolite, inhibits tubulin polymerization by acting at the colchicine site. Proc Natl Acad Sci U S A 1994;91:3964–8.

5. Hamel E, Lin C, Flynn E, D'Amato R. Interactions of 2-methoxyestradiol, an endogenous mammalian metabolite, with unpolymerized tubulin and with tubulin polymers. Biochem J 1996;35:1304–10.

6. Mabjeesh NJ, Escuin D, LaVallee TM, et al. 2-ME2 inhibits tumor growth and angiogenesis by disrupting microtubules and dysregulating HIF. Cancer Cell 2003;3:1–13.

7. Attalla H, Makela T, Adlercreutz H, Andersson L. 2-Methoxyestradiol arrests cells in mitosis without depolymerizing tubulin. Biochem Biophys Res Commun 1996;228:467–73.

8. Sattler M, Quinnan LR, Pride YB, et al. 2-Methoxyestradiol alters cell motility, migration and adhesion. Blood 2003;102:289–96.

9. Mitchison TJ, Kirschner M. Dynamic instability of microtubule growth. Nature 1984;312:237–42.

10. Cassimeris L. Accessory protein regulation of microtubule dynamics throughout the cell cycle. Curr Opin Cell Biol 1999;11:134–41.

11. Jordan MA. Mechanism of action of antitumor drugs that interact with microtubules and tubulin. Curr Med Chem Anti-Canc Agents 2002;2:1–17.

12. Grishchuk EL, Molodtsov MI, Ataullakhanov FI, McIntosh JR. Force production by disassembling microtubules. Nature 2005;438:384–8.

13. Rudner AD, Murray AW. The spindle assembly checkpoint. Curr Biol 1996;8:773–80.

14. Jordan MA, Thrower D, Wilson L. Effects of vinblastine, podophyllotoxin and nocodazole on mitotic spindles. Implications for the role of microtubule dynamics in mitosis. J Cell Sci 1992;102:401–16.

15. Dhamodharan RI, Jordan MA, Thrower D, Wilson L, Wadsworth P. Vinblastine suppresses dynamics of individual microtubules in living cells. Mol Biol Cell 1995;6:1215–29.

16. Wilson L, Miller HP, Farrell KW, Snyder KB, Thompson WC, Purich DL. Taxol stabilization of microtubules *in vitro*: dynamics of tubulin addition and loss at opposite microtubule ends. Biochemistry 1985;24:5254–62.

DOI:10.1158/1535-7163.MCT-06-0113

17. Toso RJ, Jordan MA, Farrell KW, Matsumoto B, Wilson L. Kinetic stabilization of microtubule dynamic instability in vitro by vinblastine. Biochemistry 1993;32:1285 – 93.

18. Bradford MM. A rapid and sensitive method for the quantitation of microgram quantities of protein utilizing the principle of protein-dye binding. Anal Biochem 1976;72:248 – 54.

19. Kamath K, Jordan MA. Suppression of microtubule dynamics by epothilone B in living MCF7 cells. Cancer Res 2003;63:6026 – 31.

20. Panda D, Goode BL, Feinstein SC, Wilson L. Kinetic stabilization of microtubule dynamics at steady state by τ and microtubule-binding domains of tau. Biochemistry 1995;34:11117 – 27.

21. Walker RA, O'Brien ET, Pryer NK, et al. Dynamic instability of individual microtubules analyzed by video light microscopy: rate constants and transition frequencies. J Cell Biol 1988;107:1437 – 48.

22. Jordan MA, Toso RJ, Thrower D, Wilson L. Mechanism of mitotic block and inhibition of cell proliferation by taxol at low concentrations. Proc Natl Acad Sci U S A 1993;90:9552 – 6.

23. Kowalski RJ, Giannakakou P, Gunasekera SP, Longley RE, Day BW, Hamel E. The microtubule-stabilizing agent discodermolide competitively inhibits the bindings of paclitaxel (Taxol) to tubulin polymers, enhances tubulin nucleation reactions more potently than paclitaxel, and inhibits the growth of paclitaxel-resistant cells. Mol Pharmacol 1997;52:613 – 22.

24. Sweeney C, Miller K, Sissons S, et al. The antiangiogenic property of docetaxel is synergistic with a recombinant humanized monoclonal antibody against vascular endothelial growth factor or 2-methoxyestradiol but antagonized by endothelial growth factors. Cancer Res 2001;61: 3369 – 72.

25. Chang P, Giddings TH, Winey M, Stearns T. epsilon-tubulin is required for centriole duplication and microtubule organization. Nat Cell Biol 2003; 5:71 – 6.